Bathymetry derived from Sentinel-1 Synthetic Aperture Radar data

Stefan Wiehle, German Aerospace Center, Henrich-Focke-Str. 4, 28199 Bremen, +49 421 24420 1863, stefan.wiehle@dlr.de, Germany
Andrey Pleskachevsky, German Aerospace Center, andrey.pleskachevsky@dlr.de, Germany

Abstract

This paper presents the use of Sentinel-1 Synthetic Aperture Radar (SAR) satellite data to derive bathymetry, the topography of the sea floor. With the growing efforts in global shipping and offshore constructions like wind parks, the knowledge of bathymetry becomes increasingly important. An automatic algorithm is used to retrieve the peak wavelengths of long swell waves from SAR acquisitions of coastal seas and calculate the bathymetry using the shoaling effect, which leads to waves becoming shorter when approaching shallower waters. The peak wave period, required for solving the dispersion relation, is also automatically retrieved by comparison to existing datasets.

1 Introduction

With the advance of satellite remote sensing technology, the continental topography can be accurately measured by Synthetic Aperture Radar (SAR) satellites, as recently done globally by the TanDEM-X mission [4]. However, about 70% of the Earth are covered by water, where the sea floor topography cannot be measured by a single spaceborne Earth Observation technology today. Conventional means of measuring the bathymetry use ship-mounted echo sounders; shallow water with low turbidity can also be covered with plane-mounted techniques like LIDAR. The high costs connected to these ways of measurement are one of major the reasons for the current lack of bathymetric data worldwide. Free datasets like GEBCO (General Bathymetric Charts of the Oceans) [2] are available, but in many areas based only on interpolation or deprecated measurement data. Even projects like EMODnet bathymetry [1], where many individual bathymetric sources are combined for European waters, still have coverage gaps.

Many of such gaps can be closed using different satellite remote sensing technologies. In shallow waters, the bathymetry can be derived from optical satellite data based on sun-light reflection analysis of the sea floor, accounting for chemical and physical characteristics of the water [9]. In deep waters several kilometers off the shore, altimeter satellite data can be used to detect underwater structures which modify the local gravity, creating a measureable change of elevation at the sea surface [10].

In this paper, a technique based on SAR satellite data is used which was presented in [7] using TerraSAR-X acquisitions. The method requires the presence of long swell waves and light to medium wind, as explained in the following section. Hence, not every SAR acquisition of coastal waters is suitable for bathymetry derivation. While TerraSAR-X offers higher resolution acquisition modes and has a better imaging of the ocean surface due to a comparably low orbit altitude, data are only available when previously ordered. Sentinel-1 data, on the other hand, is acquired constantly and fully accessible from the Copernicus data hub, which simplifies the retrieval of suitable scenes worldwide. To make use of this, the algorithm was since extended to work on Sentinel-1 data and run automatically.

2 Method

The principal method used here was presented in [7]. It requires long swell waves because of the shoaling effect, which causes changes in wavelength and wave height when the underlying topography changes. This effect occurs in waters with depths of less than half of one wavelength, approximately, where the waves interact with the seafloor.

The detection of sea surface phenomena by SAR is dependent on the availability of wind [5], which is present in oceanic scenarios most of the time. Even very low wind speeds, about $2\,\mathrm{m/s}$, are sufficient to create ripple waves, centimetre-sized distortions of the otherwise smooth water surface [8]. The characteristics of the radar echo averaged over a subscene can directly be related to wind speed and local variation of intensity can be related to wave height by image spectra analysis [6]. When swell waves, reaching wavelengths of up to several hundred meters, and ripple waves are present, the swell waves are visible on the SAR image as regular brightness modulations. Too strong local wind speeds, however, may cause white capping and wave breaking, which is seen as strong smearing in the SAR image, so the individual wave crests can no longer be discrimated. Hence, detecting wavelengths is possible for low to medium wind speeds only. Very shallow waters lead to increased wave steepening and finally breaking, which means depths below about $10\,\mathrm{m}$ are also not suitable for this type of analysis.

Swell waves are a result of distant winds and can travel several thousand kilometres across the ocean. A swell system usually has an extension of many kilometres parallel and perpendicular to the wave direction and becomes more homogenous in wavelength with increasing distance from its origin [3], hence, the incoming swell waves in deep water are considered as monochromatic in this analysis.

Using a linear approach and neglecting local circulation currents, the connection between peak wavelengths and depth is described by the rearranged dispersion relation [7]

$$d = \frac{L_p}{2\pi} \tanh^{-1}\left(\frac{2\pi L_p}{g T_p^2}\right) \quad , \qquad (1)$$

where d is the water depth, $\omega_p = 2\pi/T_p$ is the peak angular wave frequency, T_p is the peak wave period, L_p is the peak wavelength and g is the gravitational acceleration. Here, the use of the general dispersion relation for all water depths is necessary, since areas with $d < 1/2L_p$, where the waves interact with the seafloor, are explicitely considered. From Eq. (1), it follows that two parameters are required to calculate the water depth: the peak wavelength L_p and the peak wave period T_p.

The retrieval of the wavelength is performed as shown in [6]: a Fast Fourier Transformation (FFT) is applied to subsets of the SAR scene, the wavelength can then be retrieved from the resulting spectrum. The wave period cannot be directly derived from the SAR scene as it lacks temporal information. It could be taken from measurement data, but these are only sparsely available and, hence, this is approach would only be suitable in limited areas. A manual way to derive the wave period is to take the retrieved wavelength in an area with constant depth in a sea chart and calculate the wave period using this depth.

This manual procedure has now been improved and automated by using an external dataset like GEBCO, which is available worldwide, as first guess for depth information. Other datasets can be used when available, for example EMODnet bathymetry data in European waters. For each FFT calculation box in the satellite scene, a range of depths is calculated by iterating through possible wave periods. The minimal wave period is calculated from Eq. (1) using the external data, while 1.5 times the minimum value was found to be sufficient as maximum investigated wave period. The optimal wave period is found using a minimum root mean square difference (RMSD) analysis of these depths to the external dataset. This provides an automatic way to determine the wave period without in-situ measurement or operator interaction.

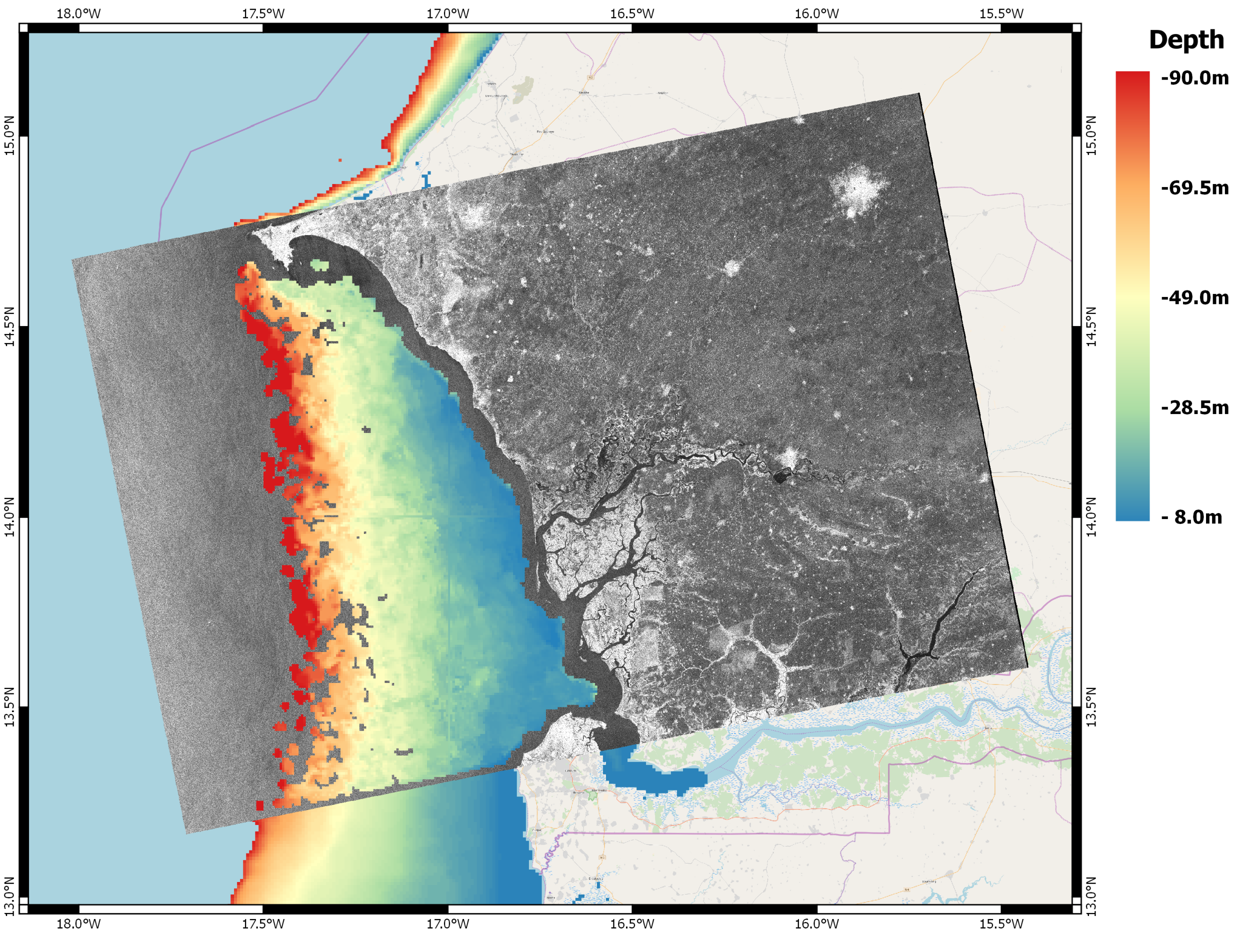

Figure 1: Retrieved bathymetry from a Sentinel-1 scene of West Africa, acquired on 2017-03-08. The colored depths within the satellite scene are retrieved by the presented algorithm, the depths shown outside the scene are from the GEBCO dataset. Background image by OpenStreetMaps.

3 Results

While the algorithm can be applied to many coastal waters worldwide, the results for an area near Dakar (West Afrika) are presented here. This section first presents the results of a single scene, followed by an analysis with multiple scenes.

3.1 Single scene

The acquisition used for this analysis is a Sentinel-1 IW scene acquired on 2017-03-08. Only the VV image is used since sea state imaged with more contrast in this mode compared to the VH image also acquired. The Sentinel-1 IW mode has a pixel spacing of $10\,\mathrm{m}$ in both directions and a swath width of $250\,\mathrm{km}$. **Figure 1** shows the retrieved depths as colored area within the Sentinel-1 scene used for the calculation. Outside of the colored areas, no depth could be retrieved as the waterdepth was too high for wave interaction or the wavelength could not be determined in the FFT subscene. The depths displayed outside the Sentinel-1 scene are from GEBCO data.

For this investigation, an FFT boxsize of $5.12\,\mathrm{km} \times 5.12\,\mathrm{km}$ was used, where the FFT boxes were arranged in an overlapping, gridded pattern offset by $700\,\mathrm{m}$ in both directions. With external data from the GEBCO 2014 dataset, the automatically retrieved wave period is $12.31\,\mathrm{s}$. The RMSD between both datasets for this wave period is $12.45\,\mathrm{m}$. Since the investigated depths are up to $90\,\mathrm{m}$, this value is within 15% accuracy. However, the GEBCO dataset used for comparison cannot be considered to contain fully accurate bathymetry in this region. Further possible sources of error that are not incorporated in the calculation are ocean currents, which change the surface wavelengths, and tidal effects changing the water level compared to values in sea charts or datasets.

3.2 Multiple scenes

In the same way as described above for the single scene, 9 other Setinel-1 IW scenes of the same area were investigated, all acquired between March 2017 and March 2018. The depth was derived at the same coordinates for each scene and the results were averaged for each coordinate. Due to differences of incoming sea state and imaging conditions, wave lengths could not be retrieved at every coordinate for each image. Only positions with at least 4 valid data points and deeper than $10\,\mathrm{m}$ were considered in the new error analysis. With 10 scenes being used and, hence, up to 10 derived depth values for each positions, the error statistics improved to an RMSD of $7.21\,\mathrm{m}$.

Figure 2 shows the difference between averaged retrieved depth and GEBCO depth; positive values indicate the GEBCO depth was deeper than the retrieved depth. In most areas, the retrieved depth is several metres deeper than the GEBCO depth. As seen along the north-eastern edge of the investigated area, the shallow waters are prone to a strong overestimation, although only areas deeper than $10\,\mathrm{m}$ were considered. On the other hand, depths in the deep waters in the west are often underestimated and strong differences are present between adjacent points. These findings are also seen in the scatterplot given in **Figure 3**, where a high spread is seen for depths of $60\,\mathrm{m}$ and above.

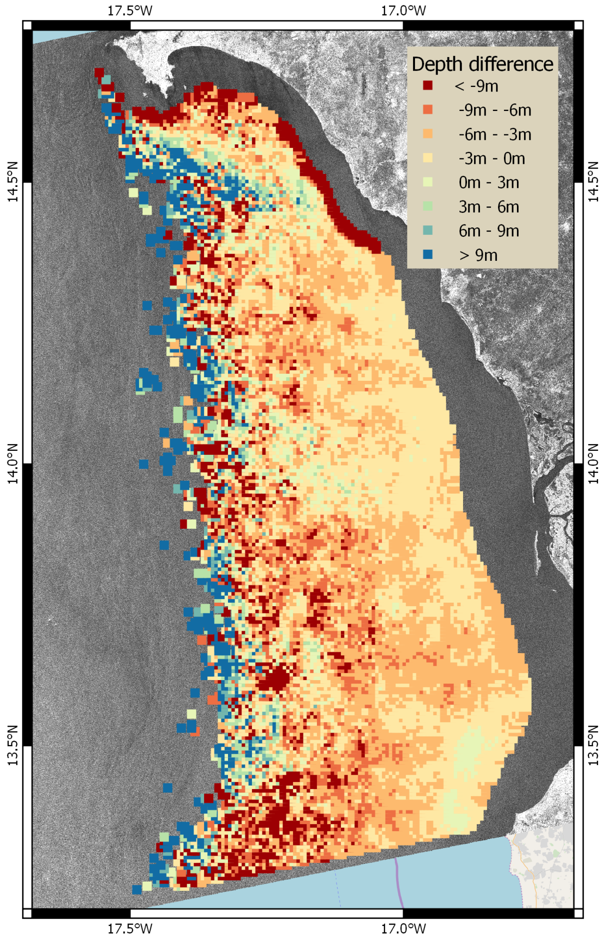

Figure 2: Difference between GEBCO data and averaged depths automatically retrieved from 10 Sentinel-1 IW acquisitions acquired between March 2017 and March 2018.

4 Conclusions

An algorithm to automatically derive the bathymetry from SAR images was developed and the results of applying it to a single scene and to multiple scenes in an area at the West African coast were presented. For the single scene, the offset to the GEBCO dataset was about 15%; a similar scope of offset was also found in other areas. Averaging multiple scenes of the same area, the RMSE reduced by more than 40%, from $12.45\,\mathrm{m}$ for the single scene to $7.21\,\mathrm{m}$ for 10 scenes. While this SAR-based bathymetry cannot match ship-based survey data in terms of accuracy and resolution, it's cheap costs make it a viable application when the requirements for accuracy and resolution are not too high, for example as a preliminary study that helps reducing the area that has to be surveyed by ships in a following multibeam campaign. The use of the method is, however, limited to coasts which regularly encounter long swell waves and have extended areas with waterdepths below 100 m. Due to the high amount of acquisitions freely available, Sentinel-1 is a good choice for global data coverage and the IW mode provides sufficient resolution for long swell waves.

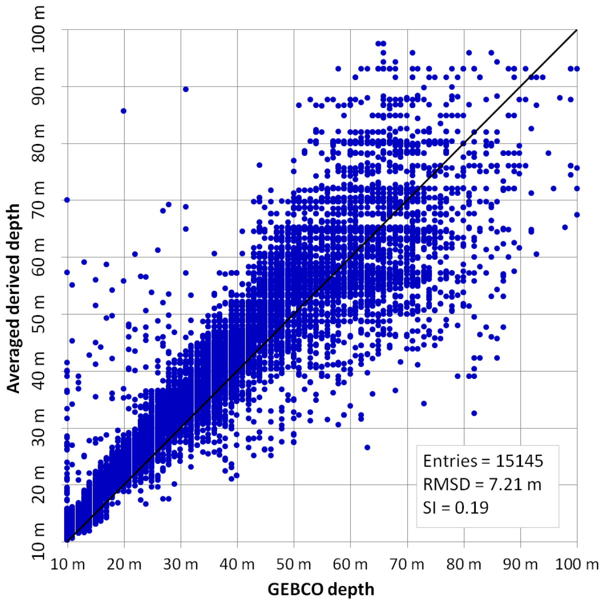

Figure 3: Scatterplot for the averaged bathymetry from 10 scenes. 15145 points were investigated, the RMSD is 7.21 m and the scatter index is 0.19.

Acknowledgements

The research leading to these results has received funding from the European Union's Horizon 2020 research and innovation programme under grant agreement No 687323.

References

[1] European Marine Observation Data Network (EMODnet) bathymetry. accessed on 2017-10-23.

[2] General Bathymetric Charts of the Oceans (GEBCO). accessed on 2017-10-23.

[3] Claus Gebhardt, Jean-Raymond Bidlot, Johannes Gemmrich, Susanne Lehner, Andrey Pleskachevsky, and Wolfgang Rosenthal. Wave observation in the marginal ice zone with the TerraSAR-X satellite. *Ocean Dynamics*, 66(6):839–852, 2016.

[4] Gerhard Krieger, Alberto Moreira, Hauke Fiedler, Irena Hajnsek, Marian Werner, Marwan Younis, and Manfred Zink. TanDEM-X: A satellite formation for high-resolution SAR interferometry. *IEEE T. Geosci. Remote*, 45(11):3317–3341, 2007.

[5] Xiaoming Li, Susanne Lehner, and Wolfgang Rosenthal. Investigation of ocean surface wave refraction using TerraSAR-X data. *IEEE T. Geosci. Remote*, 48(2):830–840, Feb 2010.

[6] A.L. Pleskachevsky, W. Rosenthal, and S. Lehner. Meteo-marine parameters for highly variable environment in coastal regions from satellite radar images. *ISPRS J Photogramm*, 119:464 – 484, 2016.

[7] Andrey Pleskachevsky, Susanne Lehner, Thomas Heege, and Claudius Mott. Synergy and fusion of optical and synthetic aperture radar satellite data for underwater topography estimation in coastal areas. *Ocean Dynamics*, 61(12):2099–2120, 2011.

[8] Johannes Schulz-Stellenfleth, Jochen Horstmann, Susanne Lehner, and Wolfgang Rosenthal. Sea surface imaging with an across-track interferometric synthetic aperture radar: the SINEWAVE experiment. *IEEE T Geosci Remote*, 39(9):2017–2028, 2001.

[9] J. Siermann, C. Harvey, G. Morgan, and T. Heege. Satellite derived bathymetry and digital elevation models (DEM). *IPTC-17346*, 2014.

[10] Walter H. F. Smith and David T. Sandwell. Global sea floor topography from satellite altimetry and ship depth soundings. *Science*, 277(5334):1956–1962, 1997.